A novel molecular probe ^{131}I-K237 targeting tumor angiogenesis in human prostate cancer xenografts

QIAN ZHAO[1], YU ZHANG[2], JUN GUO[3] and JUAN LI[1]

[1]Department of Nuclear Medicine, General Hospital of Ningxia Medical University, Yinchuan, Ningxia 750004;
[2]Department of Nuclear Medicine, Affiliated Hospital of Luzhou Medical College, Luzhou, Sichuan 646000;
[3]Department of Nuclear Medicine, Postgraduate College of Ningxia Medical University, Yinchuan, Ningxia 750004, P.R. China

Received March 29, 2014; Accepted January 21, 2015

DOI: 10.3892/mmr.2015.3504

Abstract. Specific molecular probes are essential for the early diagnosis of prostate cancer. In addition, peptides have been shown to have numerous uses as diagnostic and therapeutic molecular probes. The K237 peptide binds to the vascular endothelial growth factor receptor with high affinity and specificity, and was predicted to have potential use as a probe in tumor angiogenesis. The overall aim of the present study was to assess the diagnostic potential of ^{131}I-K237 as a molecular probe for prostate cancer. The K237 peptide was radiolabeled with ^{131}I using an Iodogen method. The radiolabeling efficiency and radiochemical purity were found to be 73.7±3.2 and 96.7±0.6%, respectively, which were determined using thin layer chromatography and high performance liquid chromatography *in vitro*. Cellular uptake and competition binding experiments were used to identify the affinity of ^{131}I-K237 to LNCaP prostate cancer cells. The binding ratio of ^{131}I-K237 to LNCaP cells in the experimental group was 95.8±1.5%, whereas the binding ratios in the 5 kBq Na^{131}I, 10 kBq Na^{131}I, 15 kBq Na^{131}I and PBS groups were 8.2±0.4, 8.3±0.2, 8.5±0.2 and 0.0%, respectively. In addition, the binding ratio of ^{131}I-K237 to LNCaP significantly decreased with the increased dose of unlabeled K237. A total of 40 male BALB/c mice with LNCaP xenografts were used for biodistribution and single photon emission computed tomography imaging analysis. An image was obtained and tumors were visible from 2 h post injection of ^{131}I-K237. In conclusion, the results of the present study showed that ^{131}I-K237 had a high affinity for LNCaP cells and may be considered as a candidate diagnostic molecular probe for prostate cancer.

Correspondence to: Professor Juan Li, Department of Nuclear Medicine, General Hospital of Ningxia Medical University, 804 Shengli Street, Yinchuan, Ningxia 750004, P.R. China
E-mail: 13909575176@126.com

Key words: ^{131}I, K237, molecular imaging, biodistribution, single photon emission computed tomography

Introduction

Prostate cancer (PCa) is the most prevalent type of cancer and the second leading cause cancer-related mortality in males (1). Early diagnosis of PCa has an important role in the therapeutic strategy and prognosis of patients (2). Molecular imaging is a method of *in vivo* visualization and measurement of molecular biological processes (3); this type of technology involves the use of nuclear medicine, along with positron emission tomography (PET) and single photon emission computed tomography (SPECT), magnetic resonance spectroscopy (MRS), optical imaging and ultrasound imaging with microbubbles. Of which, PET and SPECT imaging demonstrate specific advantages (4).

Radionuclide imaging techniques, including SPECT, SPECT/CT, PET and PET/computed tomography (CT), have critical roles in the clinical diagnosis and treatment of cancer (5). Therefore, a number of studies have focused on the development of novel radiotracers for tumor angiogenesis (6-8).

Small peptides have been shown to have important advantages in cancer diagnosis and therapy, as they may be prepared through chemical synthesis, which is relatively inexpensive, and have a low risk of inducing immunogenic responses and rapid blood clearance (9).

Small peptides, which target tumor angiogenesis, may be labeled with radionuclide and used in the targeted diagnosis and therapy of PCa. Through targeted radiation, the formation of novel tumor vessels may be inhibited, which may therefore prevent further cancer progression. Hetian *et al* (10) reported that the K237 peptide, which was isolated from a phage-displayed peptide library, was able to bind to the vascular endothelial growth factor (VEGF) receptor kinase insert domain receptor/fetal liver kinase 1 (KDR) with high affinity and specificity (10).

However, there have been limited studies into diagnostic imaging and therapeutic experiments on prostate cancer with radioiodine-labeled (^{131}I)-K237.

In the present study, to the best of our knowledge, ^{131}I-K237 was used in the LNCaP prostate cancer cell line, for the first time. In addition, SPECT/CT imaging was used to characterize biodistribution of ^{131}I-K237 in prostate cancer xenografts *in vivo*. Therefore, the present study aimed to determine the

diagnostic potential of ^{131}I-K237 as a molecular probe for prostate cancer.

Materials and methods

Ethics statement. All animal experiments were approved by Ningxia Medical University Animal Studies Committee (Ningxia, China), according to the Guidelines for the Care and Use of Research Animals (Ningxia Medical University). Mice were fed a standard diet and were housed in a standard specific pathogen-free environment, with free access to food and drinking water according to the guidelines. Mice were finally sacrificed by cervical dislocation under anesthesia (0.1 ml Chloral Hydrate; Yulong Co., Ltd., Qingdao, China) to limit suffering.

Radiosynthesis of ^{131}I-K237. All chemicals used were of analytical grade and commercially available. The K237 peptide (H-His-Thr-Met-Tyr-Tyr-His-His-Tyr-Gln-His-His-Leu-OH) was synthesized through the solid-phase peptide synthesis (SPPS) method (11). K237 was radiolabeled with iodine-131 using the Iodogen method as described previously (12). The radiolabeling yields and radiochemical purity of ^{131}I-K237 were determined using thin layer chromatography (TLC) analysis using silica gel GF-254 (Qingdao Jitai Silica Gel Desiccant, Qingdao, China) coated on glass plates. Following development and drying, the plates were cut into sections and the radioactivity of each section was counted using a γ-well counter (Wizard2 Automatic Gamma Counter; PerkinElmer, Waltham, MA, USA).

A total of 30 μl of 0.1% trifluoroacetic acid (TFA; mobile phase A) and 10 μl of 10^{-3} M diethylene triamine pentaacetic acid were added together with 2 μl labeled peptide solution. High performance liquid chromatography (HPLC) analysis involved a gradient elution performed on the Agilent HPLC system 1100 Series (Agilent Technologies, Santa Clara, CA, USA) equipped with a LichroCART 250-3 LiChrospher 100 RP-18 (5 μm; Merck KGaA, Darmstadt, Germany) with a UV monitor (LB506C; Bio-Rad Laboratories, Inc., Hercules, CA, USA) and a radioactivity monitoring analyzer (B3110; Shimadzu, Tokyo, Japan) in 0.1% TFA in water as a mobile phase A and 0.1% TFA in CH_3CN as phase B. The flow rate was 1 ml/min.

Cell culture. The human LNCaP prostate cancer cell line (No. CRL-1740; American Type Culture Collection, Manassas, VA, USA) was used in this study, which was provided by the Department of Urology, General Hospital of Ningxia Medical University. LNCaP cells were grown in RPMI-1640 medium (Sigma-Aldrich, St. Louis, MO, USA) supplemented with 10% fetal bovine serum (Sigma-Aldrich) and 1 mM glutamine (Sigma-Aldrich), and cultured in a humidified atmosphere with 95% air and 5% CO_2 at 37˚C. The experiments were performed with cells in the logarithmic phase of growth. The cell growth status was monitored using inverted microscopy with phase contrast (CKX31; Olympus Corp., Tokyo, Japan).

^{131}I-K237 binding experiment. Cellular uptake and competition binding experiments were used to identify the affinity of ^{131}I-K237 to LNCaP cells. Cells were separated into groups as follows: Experimental group, treated with ^{131}I-K237; negative groups, treated with different doses of Na^{131}I; blocking groups, treated with ^{131}I-K237 and various doses of K237; and the blank group, treated with phosphate-buffered saline (PBS).

LNCaP cells were cultured in 96-well plates ($5x10^5$ per well). Cells were starved for 16 h in serum-free medium, then each group was co-cultured with different media as follows: Experimental group contains 15 kBq ^{131}I-K237 per well, the negative groups were treated with 5, 10 and 15 kBq Na^{131}I, and the blank group was treated with PBS only. Blocking groups treated with various doses of unlabeled K237 (0, 1, 2, 4, 8 and 16 μg/μl) were also added into the wells. The medium (non-uptake ^{131}I-K237) and cells (uptake ^{131}I-K237) of each well were then harvested at 48 h, and radioactivity was measured using the γ-well counter along with a standard, which contained 15 kBq ^{131}I. Treatment for each well was repeated three times). The cellular binding ratios were then calculated separately. The binding ability of ^{131}I-K237 was represented by the ratio of mean uptake as follows: Uptake ratio=uptake counts/mean total counts (uptake + non-uptake counts) x 100.

Biodistribution. Male BALB/c nu/nu mice (18±2 g, three weeks old; Vital River Laboratory Animal Technology Co. Ltd, Beijing, China) were use in the present study. The mice were inoculated with $1x10^7$ LNCaP cells in their right upper limb and the tumors were allowed to grow to ~0.7 cm diameter, as measured using calipers.

A total of 35 BALB/c mice with LNCaP xenografts were randomly divided into seven groups (n=5). ^{131}I-K237 was purified and isolated using HPLC analysis, as described above. A dose of 2.96 MBq ^{131}I-K237 was injected into each mouse via the lateral tail vein; all injections were successful with no leakage. The mice were then sacrificed by cervical dislocation at 30 min, 1, 2, 4, 8, 12 and 24 h following injection.

Mice were dissected and tissues of interest (blood, heart, liver, spleen, lung, kidneys, muscle and tumor) were weighed, and their radioactivity was measured using the γ-well counter (6H4/5), which was equipped with an NaI(Tl) crystal detector and coupled to a high gain photomultiplier for a maximum efficiency of 80%, along with a standard solution of the injection. Radioactivity results were recorded as the percentage injected activity per gram (%ID/g) of tissue corrected for background and decay.

SPECT imaging. A total of five BALB/c mice with LNCaP xenografts were used for SPECT; 5.55 MBq ^{131}I-K237 was injected into each mouse via the lateral tail vein. SPECT imaging was performed using a Symbia SPECT/CT imaging system equipped with a high-energy, high-resolution, parallel-hole collipator (Siemens Healthcare, Erlangen, Germany) at 1, 2, 4 and 8 h following injection; these procedures were performed at the Department of Nuclear Medicine, General Hospital of Ningxia Medical University. Images were acquired at 200,000 counts with a zoom factor of 2.0, and were digitally stored in a 64x64 pixel matrix size.

Statistical analysis. SPSS 17.0 software (SPSS Inc., Chicago, IL, USA) was used for statistical analysis. Values are presented

Table I. Biodistribution of ^{131}I-K237 in mice bearing LNCaP xenografts.

	Radioactivity at varying time points following injection of ^{131}I-K237 (%ID/g)						
Organ/tissue	30 min	1 h	2 h	4 h	8 h	12 h	24 h
Blood	15.97±0.99	9.48±1.00	8.26±0.62	5.40±0.38	1.85±0.22	1.33±0.21	0.42±0.08
Heart	6.73±0.74	4.35±0.70	2.92±0.77	2.19±0.51	1.22±0.10	0.82±0.04	0.61±0.04
Spleen	4.67±0.37	3.74±0.27	3.39±0.34	2.33±0.23	1.36±0.21	0.78±0.02	0.54±0.02
Liver	7.15±0.60	5.61±0.80	5.36±0.91	3.13±0.79	1.20±0.16	0.79±0.03	0.56±0.04
Lung	5.90±0.61	4.26±0.43	2.89±0.50	1.61±0.33	1.16±0.20	0.68±0.06	0.27±0.02
Kidney	24.03±1.78	14.13±1.82	12.14±2.30	5.51±1.34	3.17±0.55	2.41±0.46	2.22±0.33
Skeletal muscle	2.52±0.30	1.53±0.24	1.27±0.25	0.94±0.15	0.58±0.06	0.33±0.03	0.12±0.01
Tumor	5.25±0.63	3.49±0.50	3.12±0.69	2.51±0.73	1.76±0.92	1.31±0.47	0.96±0.27
Tumor/muscle	2.08±0.15	2.28±0.10	2.45±0.13	2.68±0.18	3.04±0.26	3.97±0.26	8.01±0.33

Values are presented as the mean ± standard deviation (n=5) and were corrected for background radioactivity and decay. %ID/g, percentage of injected radioactivity per gram organ or tissue; ^{131}I-K237, ^{131}I-radiolabeled K237 peptide.

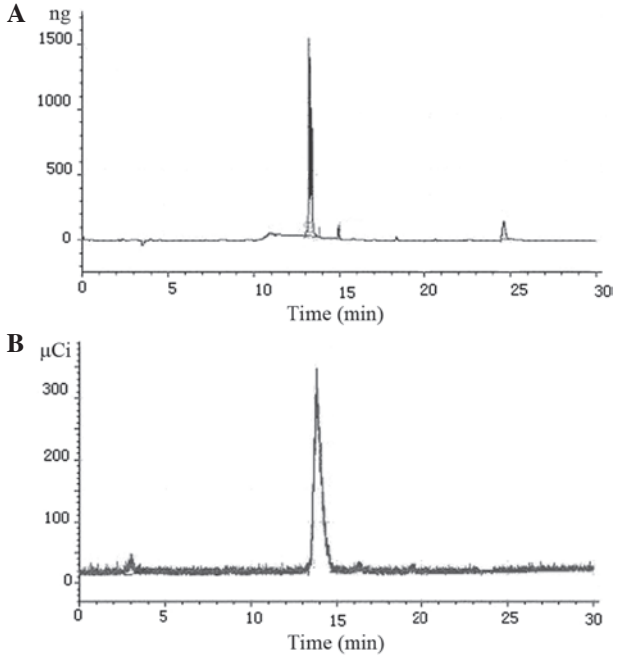

Figure 1. HPLC chromatograms of ^{131}I-K237 performed with an RP-18 column. HPLC analysis revealed that the radiochemical purity of ^{131}I-K237 was 98.3%. (A) UV detection showed that the chromatographic peak of ^{131}I-K237 appeared at 13.27 min; and (B) radiation detection showed that the radiation peak of ^{131}I-K237 appeared at 13.8 min. The time difference between the chromatographic and radiation peak occurred due to the sample flowing through the UV detection first. HPLC, high-performance liquid chromatography; UV, ultraviolet; ^{131}I-K237, ^{131}I-radiolabeled K237 peptide.

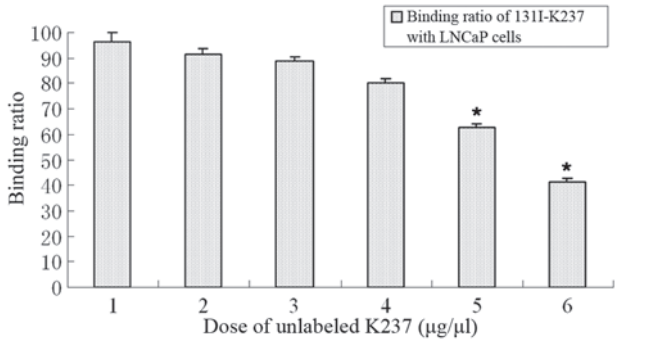

Figure 2. Binding ratio of ^{131}I-K237 to LNCaP cells. Increasing doses of unlabeled K237 induced a significant decrease in the binding ratio of ^{131}I-K237. Values are presented as the mean ± standard deviation (n=5; *P<0.05 compared with groups 1-4). 1-6, 0, 1, 2, 4, 8 and 16 μg/μl, respecively. ^{131}I-K237, ^{131}I-radiolabeled K237 peptide.

as the mean ± standard deviation and a one-way analysis of variance was used to determine differences among groups. P<0.05 was considered to indicate a statistically significant difference.

Results

Radiosynthesis of ^{131}I-K237. TLC was used to monitor the radiolabeling yields of ^{131}I-K237. The radiolabeling yield was found to be 73.7±3.2% and the optimum radiolabeling conditions occurred when cells were treated with 100 μg K237 and 50 μg Iodogen with a reaction duration and temperature of 40 min and 37˚C, respectively. Radiochemical purities of >98.3% were obtained following purification. A representative example of HPLC analysis of the selected radiolabeled peptide is shown in Fig. 1.

^{131}I-K237 binding affinity for LNCaP cells. The binding ratio of ^{131}I-K237 to LNCaP cells in the experimental group was 95.8±1.5%, whereas the binding ratio in the 5 kBq Na^{131}I, 10 kBq Na^{131}I, 15 kBq Na^{131}I and PBS groups were 8.2±0.4, 8.3±0.2, 8.5±0.2 and 0±0%, respectively. Conversely, the binding ratio of ^{131}I-K237 to LNCaP cells significantly declined with the increased dose of unlabeled K237 (Fig. 2).

Biodistribution of ^{131}I-K237 in mice bearing LNCaP xenografts. Biodistribution data are shown in Table I. The biodistribution of ^{131}I-K237 was found to be characterized by rapid blood clearance, with 15.97 %ID/g remaining at 30 min following injection of 2.96 MBq ^{131}I-K237, which

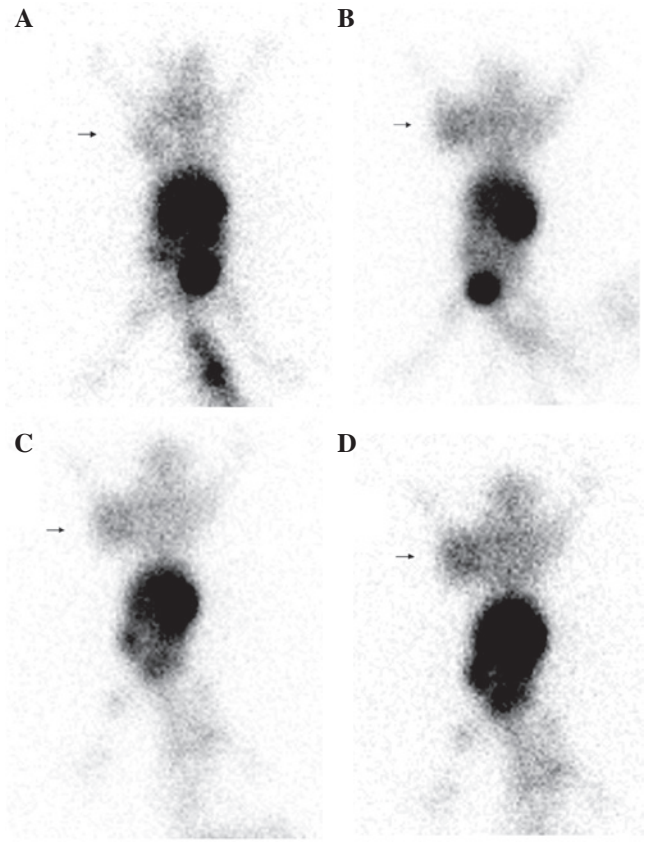

Figure 3. ^{131}I-K237 SPECT imaging in LNCaP prostate cancer xenograft mouse models. SPECT images were obtained at (A) 1, (B) 2, (C) 4 and (D) 8 h post-injection of ^{131}I-K237. Tumors on the front right upper extremities were observed at 2 h and were clearly visible at 4 h post injection. Arrows indicate the tumors. ^{131}I-K237, ^{131}I-radiolabeled K237 peptide; SPECT, single photon emission computed tomography.

was reduced to 1.85 %ID/g by 8 h post injection. In addition, the uptake of ^{131}I-K237 in the tumor remained at a relatively high level until 24 h following injection. As a result, the ratio of tumor-to-muscle (T/M) ^{131}I-K237 accumulation markedly increased in a time-dependent manner. Notably, the T/M ratio reached 8.01±0.33 by 24 h post injection.

SPECT imaging of LNCaP xenografts in mice following treatment with ^{131}I-K237. As shown in Fig. 3, nude mice bearing LNCaP xenografts were injected with 5.55 MBq ^{131}I-K237 and SPECT imaging was performed at 1, 2, 4 and 8 h following injection. Tumors were observed at 2 h and were clearly visible by 4 h post injection of ^{131}I-K237; this therefore indicated that the concentration of ^{131}I-K237 in tumors gradually increased in a time-dependent manner.

Discussion

An increasing number of studies have started to focus on the targeted diagnosis and therapy of PCa (13-15) and it is essential to identify effective and specific targets involved in the formation and metastasis of PCa. It has been well-documented that tumor angiogenesis has a vital role in tumor growth and the initiation of metastasis (16-19). VEGF has been demonstrated to act as an endothelial cell-specific mitogen and has been confirmed to have a critical role in tumor angiogenesis (20,21). In addition, the binding of VEGF and its receptor KDR has been reported to initiate the downstream effect of neovascularization (22).

The K237 peptide (HTMYYHHYQHHL), which was found to be involved in preventing the binding of VEGF to KDR, was isolated from the screening phage-displayed peptide library (10). K237 not only competed with VEGF in binding to KDR, but also specifically inhibited human endothelial cell proliferation *in vitro* (10). Therefore, the peptide K237 was shown to be an effective antagonist of VEGF. Furthermore, K237 was reported to inhibit tumor angiogenesis as well as reduce tumor growth and metastasis (23).

In the present study, K237 was radiolabeled (^{131}I-K237) and the potential applications of ^{131}I-K237 SPECT imaging were investigated, which were found to target tumor angiogenesis in PCa xenografts in mice (23).

Radiolabeled molecules have important roles in elucidating tumor status and characteristics, including aggressiveness and angiogenesis, as well as roles in monitoring the effectiveness of cancer treatments, including chemotherapy and radiotherapy (24). In the present study, the radiolabeling yield of ^{131}I-K237 was found to be 73.7±3.2%, as determined using the Idogen method, which was higher compared with that of a study by Wang *et al* (25).

The results of the present study showed that ^{131}I-K237 had a high affinity for LNCaP cells, which had a binding ratio of 95.8±1.5%; this result was comparable with that of a study by Wei *et al* (26). In the present study, the binding ratio of Na^{131}I groups were <10%, which confirmed that the higher affinity of the experimental group did not occur due to the contribution of radioiodine-131. In the blocking groups, the affinity of ^{131}I-K237 for LNCaP cells declined with the increased dose of unlabeled K237. This, therefore, suggested that unlabeled K237 was able to compete for binding sites with ^{131}I-K237, and this showed the binding specificity of ^{131}I-K237.

In the present study, the biodistribution data for nude mice bearing LNCaP xenografts indicated that there was a rapid tumor uptake of ^{131}I-K237. In addition, rapid blood clearance was demonstrated, with >66% of the tracer cleared by 4 h post injection. By contrast, the concentration of ^{131}I-K237 in tumors was relatively high compared with other tissues, with 3.49 %ID/g remaining at 1 h and 2.51 %ID/g remaining at 4 h. In addition, a high ratio of T/M was demonstrated at different time-points; notably, the T/M ratio reached 8.01±0.33 by 24 h post injection.

The rapid blood clearance and high tumor uptake observed in the present study was comparable with that in a previous study on a tumor angiogenesis-specific ^{131}I-radiolabeled RRL peptide (27).

SPECT is a powerful technique for taking low-level nuclear measurements (28). In the present study, the imaging value of ^{131}I-K237 in LNCaP xenografts was investigated. ^{131}I targeted via K237 generated clear radioactivity accumulations in prostate cancer xenografts, as determined using SPECT imaging. The tumors were clearly visible and radiotracer accumulation was also observed in the kidneys, which correlated with the results of biodistribution determination.

In conclusion, the results of the present study demonstrated that ^{131}I-K237 may be a promising imaging agent with diagnostic and therapeutic value in prostate cancer. Therefore, ^{131}I-K237 has the potential for use as a probe for the detection of prostate cancer *in vivo*.

Acknowledgements

The present study was supported by grants from The Natural Science Foundation of Ningxia (no. NZ10140) and the Research Fund of Ningxia Medical University (no. XT201320). The authors would like to acknowledge the contributions of the research groups of the Departments of Nuclear Medicine at the General Hospital of Ningxia Medical University and Affiliated Hospital of Luzhou Medical College.

References

1. Siegel R, Naishadham D and Jemal A: Cancer statistics, 2013. CA Cancer J Clin 63: 11-30, 2013.
2. da Silva HB, Amaral EP, Nolasco EL, *et al*: Dissecting major signaling pathways throughout the development of prostate cancer. Prostate cancer 2013: 920612, 2013.
3. Weissleder R and Pittet MJ: Imaging in the era of molecular oncology. Nature 452: 580-589, 2008.
4. Macis G, Di Giovanni S, Di Franco D and Bonomo L: Future perspectives for diagnostic imaging in urology: from anatomic and functional to molecular imaging. Urologia 80: 29-41, 2013 (In Italian).
5. Wagner HN Jr: Advancing a molecular theory of disease. J Nucl Med 49: 15N-34N, 2008.
6. Engle JW, Hong H, Zhang Y, Valdovinos HF, Myklejord DV, *et al:* Positron emission tomography imaging of tumor angiogenesis with a 66Ga-labeled monoclonal antibody. Mol Pharm 9: 1441-1448, 2012.
7. Haubner R and Decristoforo C: Radiolabelled RGD peptides and peptidomimetics for tumour targeting. Front Biosci (Landark Ed) 14: 872-886, 2009.
8. Liu S, Liu H, Jiang H, Xu Y, Zhang H and Cheng Z: One-step radiosynthesis of ^{18}F-AlF-NOTA-RGD$_2$ for tumor angiogenesis PET imaging. Eur J Nucl Med Mol Imaging 38: 1732-1741, 2011.
9. Perugini M, Varelias A, Sadlon T and D'Andrea RJ: Hematopoietic growth factor mimetics: from concept to clinic. Cytokine Growth Factor Rev 20: 87-94, 2009.
10. Hetian L, Ping A, Shumei S, *et al*: A novel peptide isolated from a phage display library inhibits tumor growth and metastasis by blocking the binding of vascular endothelial growth factor to its kinase domain receptor. J Biol Chem 227: 43137-43142, 2002.
11. Shelton PT and Jensen KJ: Linker, resins, and general procedures for solid-phase procedures for solid-phase peptide synthesis. Methods Mol Biol 1047: 23-41, 2013.
12. Salacinski RP, McLean C, Sykes JE, *et al:* Iodination of proteins, glycoproteins, and peptides using a solid-phase oxidizing agent 1,3,4,6-tetrachloro-3α-6α-diphenyl glycouril (Iodogen). Anal Biochem 117: 136-146, 1981.
13. Auprich M, Bjartell A, Chun FK, *et al*: Contemporary role of prostate cancer antigen 3 in the management of prostate cancer. Eur Urol 60: 1045-1054, 2011.
14. Ren J, Wang F, Wei G, *et al*: MRI of prostate cancer antigen expression for diagnosis and immunotherapy. PLoS One 7: e38350, 2012.
15. Mease RC, Foss CA and Pomper MG: PET imaging in prostate cancer: focus on prostate-specific membrane antigen. Curr Top Med Chem 13: 951-962, 2013.
16. Folkman J: Role of angiogenesis in tumor growth and metastasis. Seminars in oncology. WB Saunders 29 (6 Suppl 16): 15-18, 2002.
17. Prud'homme GJ and Glinka Y: Neuropilins are multifunctional coreceptors involved in tumor initiation, growth, metastasis and immunity. Oncotarget 3: 921-939, 2012.
18. Cai Y, Balli D, Ustiyan V, *et al*: Foxm1 expression in prostate epithelial cells is essential for prostate carcinogenesis. J Biol Chem 288: 22527-22541, 2013.
19. Li R, Ren M, Chen N, *et al*: Presence of intratumoral platelets is associated with tumor vessel structure and metastasis. BMC Cancer 14: 167, 2014.
20. Roskoski R Jr: Vascular endothelial growth factor (VEGF) signaling in tumor progression. Crit Rev Oncol Hematol 63: 179-213, 2007.
21. Dai J and Rabie AB: VEGF: an essential mediator of both angiogenesis and endochondral ossification. J Dent Res 86: 937-950, 2007.
22. Zheng Q, Du J, Zhang Z, *et al*: Association study between of Tie2/angiopoietin-2 and VEGF/KDR pathway gene polymorphisms and vascular malformations. Gene 523: 195-198, 2013.
23. Zhang YL, Wang P, Lu YY, *et al*: Effects of K237 on the proliferation of PC-3M cells and mRNA expressions of bax and bcl-2. Zhonghua Nan Ke Xue 15: 1098-1101, 2009 (In Chinese).
24. Al-Saeedi FJ, Bitar M and Pariyani S: Effect of asiaticoside on 99mTc-tetrofosmin and 99mTc-sestamibi uptake in MCF-7 cells. J Nucl Med Technol 39: 279-283, 2011.
25. Wang H, Xia JW, Zhang ZY, *et al:* Preparation of ^{131}I-K237 and the experimental study on targeting therapy in nude mice bearing human lung cancer. Chinese J Nucl Med 30: 390-394, 2010 (In Chinese).
26. Wei H, Hao X and Su M: Study on the affinity of peptides K237 with human prostate cancer cell line LNcap. Mod Oncol 15: 10-12, 2007 (In Chinese).
27. Zhao Q, Yan P, Yin L, *et al:* Validation study of 131I-RRL: Assessment of biodistribution, SPECT imaging and radiation dosimetry in mice. Mol Med Rep 7: 1355-1360, 2013.
28. Burnett JL and Davies AV: Investigating the time resolution of a compact multidimensional gamma-spectrometer. J Radioanal Nucl Chem 288; 699-703, 2011.